KSCE Journal of Civil Engineering (2017) 00(0):642-651
DOI 10.1007/s12205-016-1365-9


*Geotechnical Engineering*
pISSN 1226-7988, eISSN 1976-3808
www.springer.com/12205

# Evaluating the Liquefaction Potential of Gravel Soils with Static Experiments and Steady State Approaches

**Jinung Do*, Seoung-Beom Heo**, Yeo-Won Yoon***, and Ilhan Chang******

Received May 6, 2015/Revised February 21, 2016/Accepted April 11, 2016/Published Online May 31, 2016

## Abstract

Liquefaction generally occurs in loose sandy soils, whereas static (*i.e.*, post) liquefaction is reported to occasionally take place in gravel soils (*i.e.*, gravel-sand mixtures). Recent studies imply specific in situ parameters such as relative density or effective stress correlate with the static liquefaction potential of gravel soils, although they are insufficient to quantitatively estimate the liquefaction potential of gravel soils. In this study, the mechanism and the phenomena of static (post) liquefaction in gravel soils have been studied in detail through laboratory experiments. A state parameter ($\psi$) has been adopted to evaluate the static liquefaction and stress variation behaviors of gravel soils for a steady state Condition. Undrained (CU) triaxial tests were performed on gravel soils with different initial densities and confinement levels. State parameters for specific gravel contents at various initial relative densities are obtained from experimental programs, and are correlated with the liquefaction resistance of gravel soils. The liquefaction potential of gravel soils is then analyzed in terms of external and internal factors. The results indicate that the state parameter is an effective indicator of static liquefaction of gravel soils.

Keywords: *liquefaction, gravel soils, static triaxial test, steady state, state parameter*

## 1. Introduction

Seismic events (*e.g.*, earthquakes) in the vicinity of loose sands could cause liquefaction due to the reduction of ground effective stress or stiffness rendered by the instantaneous undrained condition and accompanying excessive pore water pressure generation in soil (Castro and Poulos, 1977; Guettaya *et al.*, 2013; Wang, 1984). Generally, liquefaction has been considered only for sandy soils (*SP* in the typically used Unified Soil Classification System (*USCS*)) or sandy soils with fines (*SM* in the *USCS*) at loose (*e.g.*, relative density ($D_r$) < 60) and undrained conditions (Ishihara, 1993; Terzaghi *et al.,* 1996), while gravel soils have been regarded as being safe from liquefaction due to their high strength and relatively large grain size (*i.e.*, $D_{50}$ > 4.75 mm), which provides proper drainage (*i.e.*, high hydraulic conductivity) conditions. In this light, application of gravel soils for embankment construction has been recommended due to their high strength and drainage characteristics, which improve resistance to liquefaction (Andrus and Chung, 1995). However, detailed evaluations and characterizations of gravel soils have not been adequately carried out due to difficulties in performing both laboratory and site explorations on stiff gravel layers (*e.g.*, insufficient performance of equipment installation) (Lin *et al.*, 2004; National Research Council, 1985).

Meanwhile, in situ liquefaction cases of gravel soils have recently been reported worldwide (Table 1). For instance, it was reported that the *Wenchuan* earthquake (China in 2008; $M_w$ = 7.9) induced liquefaction at 118 sites in *Sichuan* province, where most sites were discovered to be loose gravelly layers (Fig. 1) (Cao *et al.*, 2011). Moreover, most cases of liquefaction in gravel soils occurred in saturated loose gravel layers nearby water (*e.g.*, reservoirs, rivers) when forced by extremely high seismic motions (*e.g.*, intensity = 7 ~ 10, $M_w$ = 6.8 ~ 9.2, $M_s$ = 7.3 ~ 8.0, and PGA = 0.05 ~ 1.2 *g*) (Table 1). Therefore, gravel soils accompany the possibility of liquefaction during or after in situ seismic motions (post-liquefaction), and further investigations should be carried out to attain a detailed understanding of the liquefaction mechanism and characteristics.

Several studies on the liquefaction behavior of gravel soils have been reported (Evans *et al.*, 1992; Evans and Zhou, 1995; Kokusho *et al.*, 2004). Evans and Zhou (1995) considered equivalent void ratios between pure sand and gravelly sands,

*Graduate Student, Dept. of Civil, Construction and Environmental Engineering, North Carolina State University, Raleigh, NC 27606, USA (E-mail: jdo@ncsu.edu)
**Executive Director, Geotechnical Engineering Research Division, Hanmac Engineering Co., Ltd., Seoul 05774, Korea (E-mail: sbhur01@naver.com)
***Member, Professor, Dept. of Civil Infrastructure Engineering, Inha University, Incheon 22212, Korea (E-mail: yoonyw@inha.ac.kr)
****Member, Senior Researcher, Geotechnical Engineering Research Institute, Korea Institute of Construction Technology (KICT), Goyang 10223, Korea (Corresponding Author, E-mail: ilhanchang@kict.re.kr)

Table 1. Case Histories of Liquefaction at Gravel Soil Sites (After Cao *et al.*, 2011 and U.S. Geological Survey)

| Year | Nation | Earthquake & Location | Strength | Features |
|---|---|---|---|---|
| 1964 | USA | Alaska | Intensity: 11; $M_w$: 9.2<br>PGA: 0.14~0.18 g | Alluvial fan; loose |
| 1975 | China | Haicheng; Shimen dam,<br>Liaoning province | Intensity: 7<br>$M_s$: 7.3 | Loose; un-compacted fill in upstream shell of dam |
| 1976 | China | Tangshan;<br>Miyun dam, Beijing | $M_w$: 7.8 | 140 sec. Loose to medium dense;<br>un-compacted fill in upstream shell of dam |
| 1976 | China | Tangshan; Luan county urban | Intensity: 10<br>$M_w$: 7.1 | Sample of ejected gravel containing large particles<br>(mostly 3 ~ 9 cm with 15 cm maximum) |
| 1976 | Italy | Friuli | $M_s$ 6.5<br>PGA 0.2 g | Alluvial fan; liquefied during two earthquake 4 month apart;<br>$V_s$ = 140 ~ 210 m/s |
| 1983 | USA | Borah Peak; Pence Ranch area | Intensity: 9; $M_w$: 6.9<br>PGA: 0.3~0.5 g | Alluvial fan; the slope is 5°; loose |
| 1993 | Japan | Hokkaido-Nansei-Oki;<br>Mt. Komagataka | $M_w$: 7.8<br>PGA: 0.5 g | $D_r$ = 30%; $D_{50}$ = 3 cm; $V_s$ = less than 100 m/s<br>(loose gravelly soils) |
| 1995 | Japan | Kobe; Port island | $M_w$: 6.8<br>PGA: 0.25~0.4 g | 12 ~ 15 m of un-compacted fill (N = 5 ~ 10)<br>overlain by 3 m of compacted fill |
| 1999 | Taiwan | Chi-Chi; Wufeng | $M_w$: 7.6~7.7; $M_s$: 7.3<br>PGA: 0.5~0.8 g | River floodplain, water table = 4.5 m;<br>loose gravelly soils located in depth of 4.5 ~ 23.5 m |
| 2008 | China | Sichuan; Wenchuan | $M_w$: 7.9; $M_s$: 8.0<br>PGA: 0.2~1.2 g | Gravelly soils with upper 3 m impermeable layer |

※$M_w$ = moment magnitude scale; $M_s$ = surface wave magnitude; PGA = peak ground acceleration.


Fig. 1. Epicenter Location of the 2008 *Wenchuan* Earthquake (*Sichuan*, China) and Cored Gravel Type Soil Samples where Liquefaction Occurred (After Cao *et al.*, 2011)

where higher liquefaction resistance for gravelly sands was obtained. Kokusho *et al.* (2004) later reported that relative density ($D_r$) governs the liquefaction resistance rather than soil type. It is thus difficult to explain the liquefaction behavior of gravel soils on the basis of soil type and composition (*e.g.*, gravel/sand/fine, relative density), and therefore a more comprehensive approach is needed to elucidate the liquefaction behavior of gravel soils.

A state parameter ($\psi$) indicates the difference between the initial ($e_o$) and steady state void ratio ($e_{ss}$) of soils subjected to large strain deformation (*i.e.*, critical state under shearing), and is given as $\psi = e_o - e_{ss}$ (Been and Jefferies, 1985). In general, the state parameter represents the current state based on the steady state (*i.e.*, critical shear strength), and it implies many physical properties such as density, compressibility, distribution, size and shape of grains, and so on (Been and Jefferies, 1985). For $\psi > 0$, soils tend to be contractive, while soils show dilative characteristics for $\psi < 0$ cases during shearing. In other words, loose soils usually have positive $\psi$ values (*i.e.*, contractive), while dense soils have negative values (*i.e.*, dilative). Cases where $\psi > 0$ thus are more critical for liquefaction considerations. Moreover, the $\psi$ value is consistent with the trend of liquefaction resistance of soils (Jefferies and Been, 2015; Santamarina and Cho, 2001).

The state parameter in static experiments thus can provide an alternative to evaluate the static liquefaction potential of soils instead of cyclic experiments. In this study, a series of static undrained experimental programs based on steady state concepts has been conducted to analyze the behavior of gravel soils. In addition, a detailed discussion elucidating the liquefaction potential of gravel soils with the state parameter is provided.

## 2. Materials and Methods

### 2.1 Tested Soils

Gravel soils were obtained from the West coast (*Incheon*) of Korea. Gravels consist of granite. For laboratory testing on gravel soils, the specimen diameter of gravel soils is recommended to be 6 to 8 times the mean size of gravel particles (Evans *et al.*, 1992; Evans and Zhou, 1995; Nicholson *et al.*, 1993). Accordingly, gravel size was chosen to be less than 6.7 mm (*i.e.*, mesh size of No. 3 sieve) on the basis of the specimen diameter (50 mm) for laboratory tests (ASTM, 2012).

*Jumunjin* sand is a standard sand in Korea, and is classified as a poorly graded sand (*SP*) with a specific gravity ($G_s$) of 2.64 and a median grain size ($D_{50}$) of 0.52 mm, and the uniformity coefficient ($C_u$) and coefficient of gradation ($C_g$) are 1.94 and 1.09, respectively. *Jumunjin* sand has a structural composition between $e_{min}$ = 0.64 and $e_{max}$ = 0.89, with an inter-particle friction angle ($\phi$) of 29.3°.

To represent 'gravel soils', specified gravel-sand mixtures were prepared with particular gravel content (GC) of 0, 20, 40, 60, 80, and 100% relative to the total weight of soil (Fig. 2). Particle size distribution curves of the gravel soils are presented in Fig. 3, and details of the geotechnical material properties are summarized in Table 2. $\gamma_{d(max)}$ and $\gamma_{d(min)}$ denote the maximum and the minimum dry density, respectively.

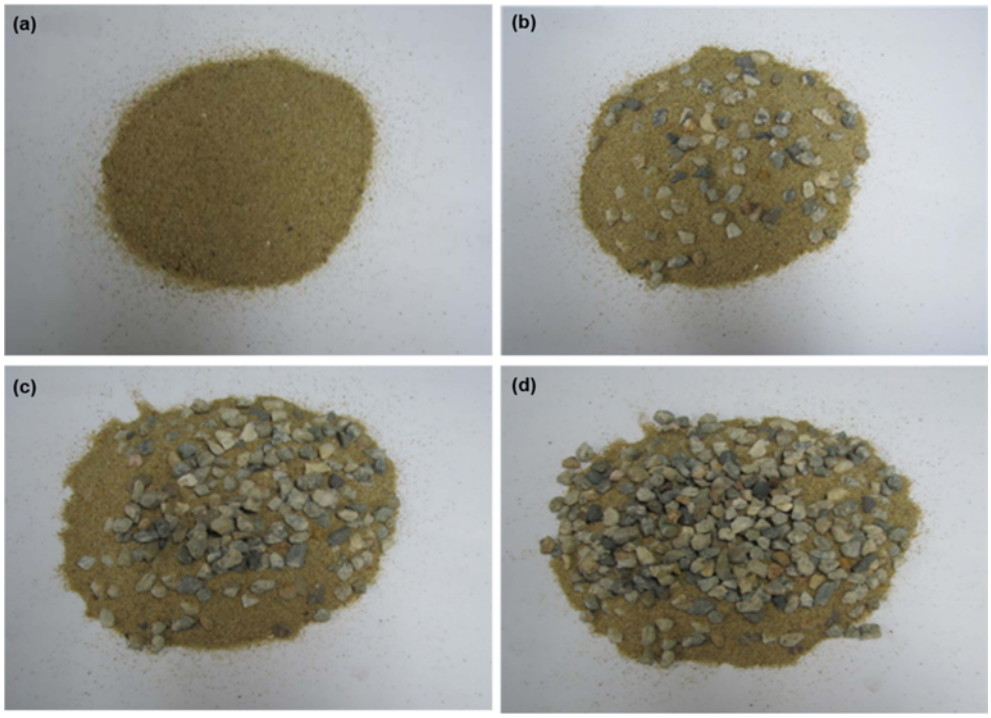


Fig. 2. Samples for Laboratory Testing: (a) GC 0%, (b) GC 20%, (c) GC 40%, (d) GC 60%

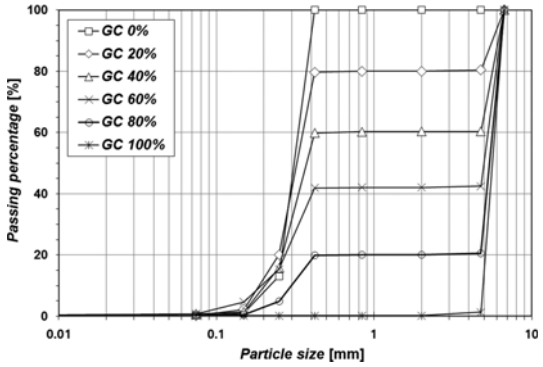


Fig. 3. Particle Size Distribution Curves with Gravel Content Variation

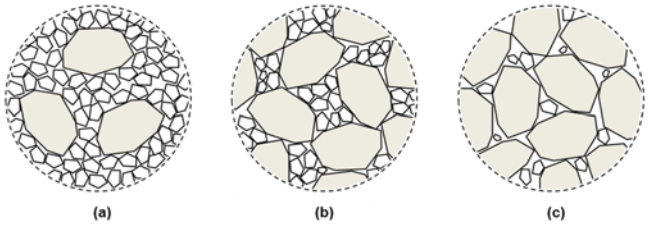


Fig. 4. Structures of Gravel-sand Mixtures: (a) GC ≪ GC for $\gamma_{max}$, (b) GC GC for $\gamma_{max}$, (c) GC ≪ GC for $\gamma_{max}$

The maximum dry density of gravel soils increases up to GC 60% and then decreases with further increases of GC (Table 2). Thus, it is regarded that gravel content between 60% ~ 70% allows complete (most compacted) gravel-sand compositions where, ideally, continuously connected gravel grains are fully filled with sand particles inside the inter-granular voids (Evans and Zhou, 1995; Kim, 2005). Consequently, this GC range results in maximum dry density ($\gamma_{max}$) of gravel soils. For GC < 60%, gravel grains are expected to be surrounded by sand particles, while sands mostly fill inter-granular voids between gravel grains for high GC (*i.e.*, GC > 60%) conditions (Fig. 4) (Siddiqi, 1984). Thus, only GC ≤ 60% conditions were considered for the laboratory experiments to represent 'generally gravel soils' rather than 'highly gravel soils' in this study. Therefore, samples transit from poorly graded sand (*SP*; GC 0, 20, and 40%) to poorly graded gravel (*GP*; GC 60%) with increasing GCs.

## 2.2 Consolidated Undrained (CU) Triaxial Test

Consolidated undrained shear triaxial tests (CU) were conducted to obtain state parameters of gravel soils using a static triaxial test device (ELE Digital Tritest 50, 25-3518/01) and applying axial strain up to 20%. Specimens were prepared by following the moist tamping method (Ladd, 1978). Gravels and sands were mixed thoroughly to prepare uniform gravel-sand mixtures. As the material properties of gravels and sands are similar (*e.g.*, $G_s$ = 2.64, $e_{min}$ = 0.63 ~ 0.64, $e_{max}$ = 0.87 ~ 0.94), it is possible to prepare uniform and well-distributed gravel-sand mixtures without any additives. To make loose samples, wet mixtures were used with 5% water content so that they could maintain their initial loose structures due to the tension and capillary force of the added water before the consolidation stage. Gravel soils with GC = 0, 20, 40, and 60% were molded into cylindrical specimens (*i.e.*, diameter 50 mm × height 100 mm) with varying initial relative density ($D_r$) conditions, and then consolidated via different isotropic confinement levels ($p_c'$) before applying deviator stresses.

Since the initial samples tended to be contracted irregularly at

Table 2. Material Properties of Gravel-sand Mixtures

| GC [%] | $C_u$ | $C_g$ | $D_{10}$ [mm] | $D_{50}$ [mm] | $\gamma_{d(max)}$ [kN/m$^3$] | $\gamma_{d(min)}$ [kN/m$^3$] | $e_{max}$ | $e_{min}$ | $e$ ($D_r$=40%) | $\gamma_{d(Dr=40\%)}$ [kN/m$^3$] | $G_s$ | USCS |
|---|---|---|---|---|---|---|---|---|---|---|---|---|
| 0* | 1.4 | 1.0 | 0.23 | 0.31 | 16.1 | 13.6 | 0.94 | 0.64 | 0.82 | 14.5 | 2.64 | SP |
| 20 | 1.5 | 1.11 | 0.21 | 0.32 | 17.31 | 14.81 | 0.78 | 0.53 | 0.68 | 15.7 | 2.64 | SP |
| 40 | 1.9 | 0.93 | 0.22 | 0.35 | 18.52 | 16.21 | 0.63 | 0.42 | 0.55 | 17.0 | 2.64 | SP |
| 60 | 27.3 | 9.4 | 0.22 | 5.00 | 19.63 | 17.34 | 0.52 | 0.34 | 0.45 | 18.2 | 2.64 | GP |
| 80 | 20 | 16.81 | 0.30 | 5.50 | 18.63 | 16.26 | 0.624 | 0.417 | 0.59 | 16.7 | 2.64 | GP |
| 100** | 1.21 | 0.97 | 4.80 | 6.00 | 16.25 | 14.09 | 0.87 | 0.63 | 0.72 | 15.1 | 2.64 | GP |

*pure sand, **pure gravel

Table 3. Summarized Conditions of the Large-strain Triaxial Tests for Gravel-sand Mixtures

| GC [%] | Initial $D_r$ [%] | $p_c'$ [kPa] | Conditions (After Consolidation) | | $e_{ss}$ | $\psi$ |
|---|---|---|---|---|---|---|
| | | | $e_o$ | $D_r$ [%] | | |
| 0 | 10 | 100 | 0.895 | 15.4 | 0.902 | -0.007 |
| | 15 | | 0.890 | 16.9 | 0.903 | -0.013 |
| | 10 | 400 | 0.864 | 25.7 | 0.856 | 0.008 |
| | 15 | | 0.832 | 36.1 | 0.856 | -0.024 |
| | 35 | | 0.821 | 39.7 | 0.856 | -0.035 |
| | 15 | 600 | 0.834 | 35.4 | 0.842 | -0.008 |
| 20 | 15 | 100 | 0.74 | 17.0 | 0.751 | -0.011 |
| | 10 | | 0.73 | 19.6 | 0.747 | -0.017 |
| | 20 | | 0.72 | 23.3 | 0.747 | -0.027 |
| | 15 | | 0.72 | 24.6 | 0.750 | -0.030 |
| | 15 | 400 | 0.70 | 30.3 | 0.701 | -0.001 |
| | 35 | | 0.69 | 36.9 | 0.708 | -0.018 |
| | 35 | | 0.67 | 43.4 | 0.704 | -0.034 |
| 40 | 10 | 100 | 0.58 | 22.0 | 0.582 | -0.002 |
| | 15 | | 0.58 | 24.6 | 0.588 | -0.008 |
| | 25 | | 0.56 | 33.0 | 0.585 | -0.025 |
| | 10 | 400 | 0.55 | 38.2 | 0.553 | -0.003 |
| | 15 | | 0.55 | 40.0 | 0.557 | -0.007 |
| | 35 | | 0.54 | 44.9 | 0.557 | -0.017 |
| 60 | 15 | 100 | 0.476 | 26.1 | 0.461 | 0.016 |
| | 10 | 400 | 0.428 | 53.7 | 0.432 | -0.004 |
| | 15 | | 0.427 | 54.0 | 0.432 | -0.005 |
| | 35 | | 0.422 | 56.8 | 0.432 | -0.010 |
| | 35 | | 0.412 | 62.4 | 0.432 | -0.020 |

the consolidation stage in accordance with the different level of confining stress, several repetitive trials were attempted to find the optimal initial relative density. In addition, specimens of GC 0%, 20%, and 40% can form loose initial structures (*i.e.*, $D_r$ = 15% ~ 40%) due to the structural composition governed by the large proportion of sands. For GC 60%, an absolute composition between gravel and sand particles results in a denser structure (*i.e.*, $D_r$ > 50%) than other GC conditions after the consolidation stage. For these reasons, non-uniform samples (*i.e.*, diverse void ratios) were prepared (Table 3).

Membrane penetration and strength correction were conducted via hydrostatic confinement and accompanying rebound measurements (Evans and Zhou, 1995). Specimens with the same $D_r$ (40%) and different GCs (*i.e.*, GC = 0% ~ 100%) were prepared. Volumetric change for a certain effective stress rebound (100 kPa → 20 kPa) has been obtained as 2.7% for GC = 100%, while a value of only 0.1 or less was obtained for other GCs (*i.e.*, GC = 0, 20, 40, and 60%). Thus, concerns about membrane penetration during testing are negligible in this study.

After consolidation, drainage was prevented (*i.e.*, turned to an undrained condition) and axial loading was applied with 1%/min strain rate (*i.e.*, 1 mm/min) up to a maximum 20% strain level. Variations of deviator stress ($q$), pore pressure ($\Delta u$), and volumetric strain ($\varepsilon_v$) were measured simultaneously during shearing. The initial void ratio ($e_o$) was obtained from a back-analysis by measuring the water content ($w$) of the specimen after testing ($S{\cdot}e_o = w{\cdot}G_s$; $S$: degree of saturation as 1.0). The mean principal stresses at 20% axial strain ($p'_{20\%}$) were taken. The steady state lines (*SSL*) for each gravel soil were then obtained as ($e_o$, log $p'_{20\%}$). Corresponding state parameter ($\psi$) values were calculated by $\psi = e_o - e_{ss}$ and analyzed for the undrained shear strength and liquefaction behavior of gravel soils.

## 3. Results and Analysis

### 3.1 Undrained Shear Behavior of Gravel Soils

The results of triaxial tests (CU) of gravel soils up to 20% axial strain are summarized in Figs. 5 and 6. Fig. 5 shows that 20% axial strain is sufficient to represent the steady state of gravel soils (Fig. 5(a)) due to the converged and constant pore water pressure condition (Fig. 5(b)), which implies that the internal stress condition remains constant ($\Delta u = q$ = constant).

The pore water pressures of gravel soils increase rapidly up to 2.5% ~ 4% strain and decrease beyond those level. This can be explained as a combination of particle densification (strain 0% ~ 4%) and volumetric expansion (*e.g.*, overturning and spinning at strain > 4%) of the gravel-sand particles (Hynes 1988). Pore water pressures of the gravel soils with GC 0, 20, and 40% show a peak value around 130 kPa, while gravel soil with GC 60% shows a higher peak pore pressure value of 180 kPa. Although the initial structure (*i.e.*, relative density) of the samples varies, it can be understood that GC 60% induces the strongest inter-granular shear resistance (Fig. 5(a)), which accompanies the highest excess pore water pressure generation (Fig. 5(b)). The results presented in Fig. 5 are in accordance with the most compacted structural composition of GC 60% (Table 2). Thus, it

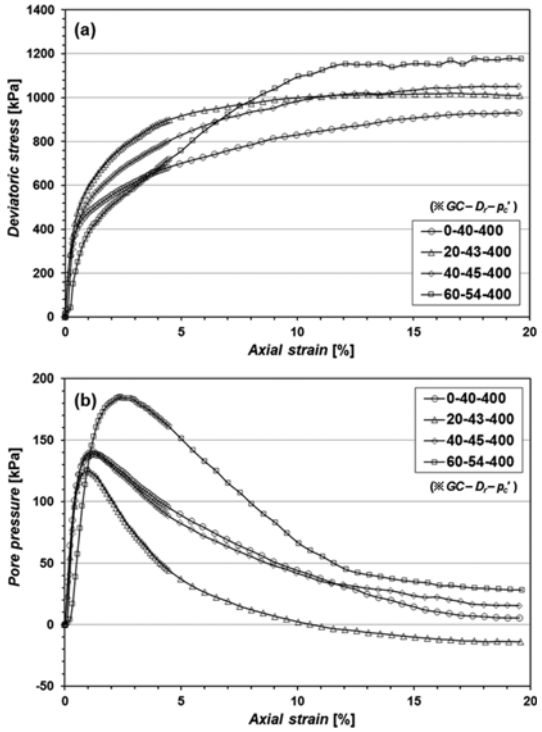


Fig. 5. Typical Pore water Pressure Behaviors with Varying Gravel Content: (a) Deviator Stress Variations, (b) Pore Pressure Variations

can be predicted that this structural characteristic will affect not only pore water pressure, but the stress behavior as well.

Figure 6 provides the mean principal effective stress ($p'$) – deviator stress ($q$) relationships normalized by the initial isotropic confining pressure ($p_c'$) with different GC values. The slope of the steady state line ($M$) for each GC was obtained via linear approximation and the friction angle at a steady state ($\phi'_{ss}$) was calculated by $M = q/p' = 6\sin\phi'_{ss} / (3 - \sin\phi'_{ss})$ (Jefferies and Been 2015). Regardless of the initial conditions (*e.g.*, relative density, confinement), each GC condition shows a single $M$ value that increases with GC increment (*i.e.*, $M = 1.29 \rightarrow 1.32 \rightarrow 1.42 \rightarrow 1.56$, for GC = 0, 20, 40, and 60%, respectively). Accordingly, the $\phi'_{ss}$ increases with GC increment (*i.e.*, $\phi'_{ss} = 32^o \rightarrow 32.8^o \rightarrow 34.9^o \rightarrow 38.2^o$), which also corresponds to strong inter-particle interactions with GC increment.

When $D_r$ is extremely low (*e.g.*, $D_r$ 26% of GC 60%; rectangular data points in Fig. 6(d)), the deviator stress at the steady state becomes even lower than the initial confinement (*i.e.*, $q/p_c' = 0.89$), which reflects the structural collapse of extremely loose gravel soils. This implies some conditions are susceptible to liquefaction even on gravel soils.

### 3.2 Steady State Line (*SSL*) Variation with Gravel Content

Figure 5 shows that 20% strain level is sufficient to represent the steady state of gravel soils, which terminates the strain hardening. Moreover, a previous study (Rahman and Lo, 2014) also used 15% and 25% strain levels as steady state points. Thus, 20% axial strain is decided to represent the steady state condition for gravel soils in this study.

To obtain the steady state line, the mean principal stresses at 20% axial strain ($p'_{20\%}$) and accompanying initial void ratios ($e_o$) are plotted together on a semi-logarithmic plane (solid dots in

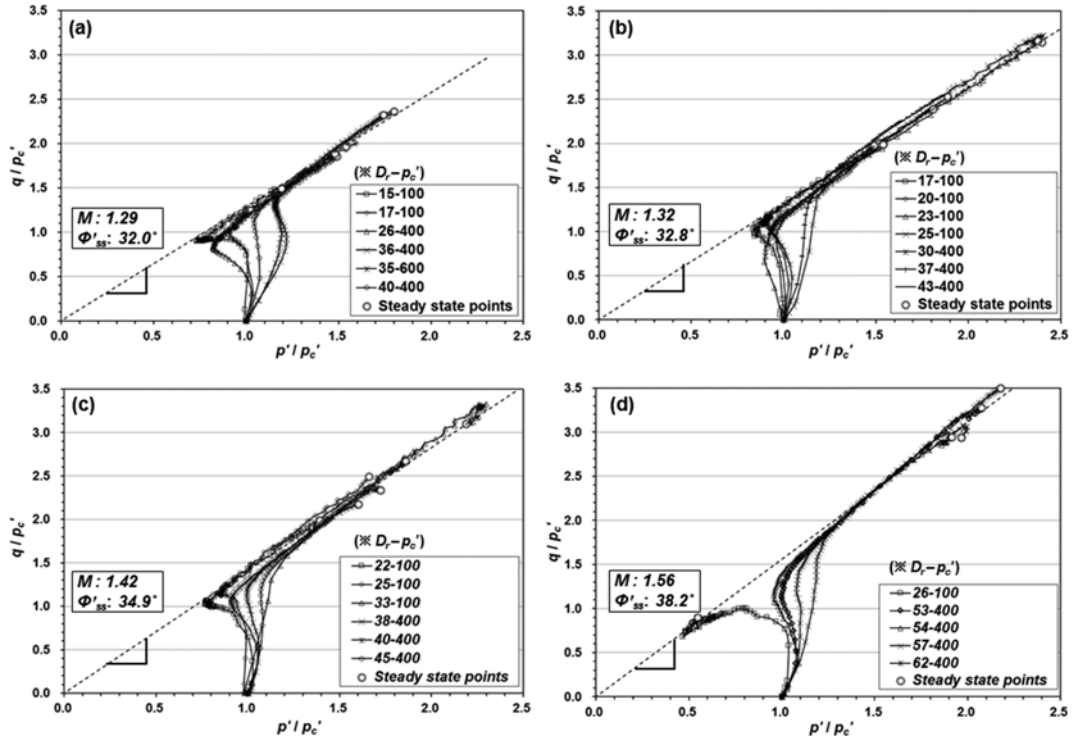


Fig. 6. Stress Behaviors with Varying Gravel Content: (a) GC 0%, (b) GC 20%, (c) GC 40%, (d) GC 60%

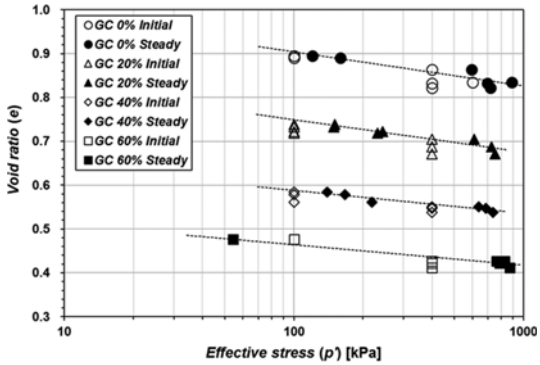


Fig. 7. Steady State Line with Varying Gravel Content

Table 4. Steady State Line Coefficients of: (a) Gravel-sand Mixtures, (b) Sand-fine Mixtures

| (a) This study | | | | (b) Jefferies and Been (2015) | | |
|---|---|---|---|---|---|---|
| Gravel content [%] | a | *b* | $R^2$ | Fine content [%] | a | b |
| 0 | -0.078 | 1.060 | 0.86 | 0 | -0.016 | 0.789 |
| 20 | -0.074 | 0.897 | 0.89 | 2 | -0.065 | 0.845 |
| 40 | -0.053 | 0.692 | 0.91 | 5 | -0.106 | 0.927 |
| 60 | -0.046 | 0.557 | 0.95 | 10 | -0.212 | 1.099 |

Fig. 7). State parameter ($\psi$) values are calculated as $\psi = e_o - e_{ss}$ for every triaxial test (Table 3). Most $\psi$ values in Table 3 are negative (–), which indicates that the gravel soils tend to be dilative when subjected to shearing or deformation.

Been and Jefferies (1985) found a linear relationship between the steady state void ratio ($e_{ss}$) and mean principal stress ($p'$) of coarse-graded soils, given as follows:

$$e_{ss} = a \cdot \log p' + b \quad (1)$$

The *a* and *b* parameters for the gravel soils in this study are summarized in Table 4. $|a|$ value indicates the slope of variation of the void ratio due to external loading (*i.e.*, $a = \Delta e/\Delta \log p'$), while the *b* parameter represents the steady state void ratio ($e_{ss}$) at extremely low confinement (*i.e.*, 1 kPa). The volume of soil changes more sensitively due to external loading for higher $|a|$ values, and a high initial void ratio is obtained with *b* increment (*i.e.*, fine sands). For example, fine-graded soils have higher $|a|$ and *b* than coarse-graded soils (Santamarina and Cho, 2001).

As shown in Table 4(a), the slope of the steady state lines ($|a|$) of gravel soils decreases slightly with increasing gravel content, which indicates the small variation of the void ratio under loading due to the strong inter-particle interlocking between gravel grains. Meanwhile, the *b* intercept decreases with GC increment, which means the natural void ratio becomes lower with GC increment up to GC 60%.

For sand-fine mixtures, the $|a|$ value increases significantly with Fine Content (FC) increment (Jefferies and Been, 2015) and becomes higher than that of gravel soils (Table 4), reflecting sensitive stress-strain characteristics of fine containing soils. A comparison between the results of this study and previous

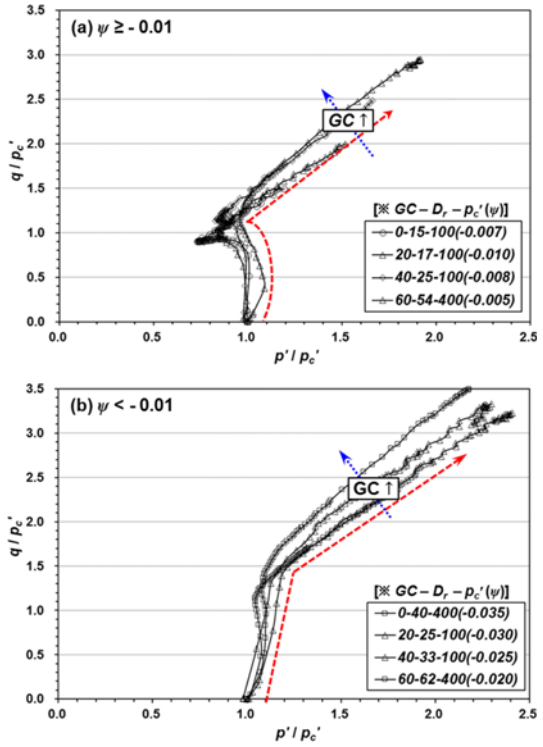


Fig. 8. Stress Behavior with Diverse Initial Conditions and State Parameters: (a) Different Initial Conditions with Similar Low $\psi$, (b) Different Initial Conditions with Similar High $\psi$

findings (Jefferies and Been, 2015) implies $|a|$ value dependency (*i.e.*, increases) with the transition of the soil composition from coarse to fine soils (*i.e.*, gravel sandy clayey soils). Thus, the gravel content and skeleton structure are dominant factors governing the steady state behavior of gravel soils.

### 3.3 State Parameter and Liquefaction Resistance of Gravel Soils

Figure 8 shows different stress paths ($p'/p_c' - q/p_c'$) depending on the state parameter ($\psi$) values. When the state parameter value is near zero (*i.e.*, $\psi \geq -0.01$), the stress paths of gravel soils show a contractive tendency, regardless of the initial relative density ($D_r$) and confinement level ($p_c'$) (Fig. 8(a)). The normalized mean principal stress ($p'/p_c'$) decreases due to volumetric contraction induced excess pore water pressure generation, which is larger than the amount of deviator stress increment at the beginning of loading. Thus, the possibility of liquefaction raises in gravel soils, even though the state parameter values are negative but close to zero ($\psi \geq -0.01$). Meanwhile, when the state parameters of gravel soils are clearly negative ($\psi < -0.01$), the stress paths of gravel soils are dilative (Fig. 8(b)). Therefore, it is concluded that there is a phase transition zone (contractive dilative) between $\psi$ near zero and $\psi < -0.01$.

As aforementioned, both the *M* and $\phi'_{ss}$ values of gravel soils increase with gravel content increment (Fig. 6). Generally, *M* becomes a function of $\phi'_{ss}$, where a single soil has an identical $\phi'_{ss}$ value regardless of the initial conditions (*e.g.*, void ratio,

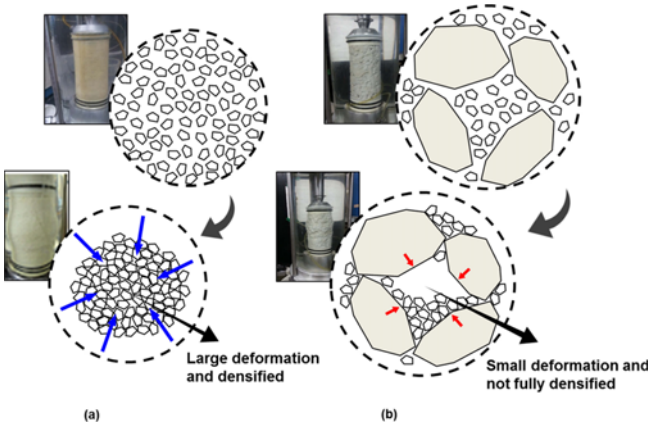


Fig. 9. Contraction Mechanism of Sand and Gravel-sand Mixtures: (a) Only Sand is Contracted Enough, (b) But Sand with Gravel is Not Contracted Enough Because of the Gravel Structures

water content) (Jefferies and Been, 2015). Thus, the increase of $M$ with higher GCs for negative state parameter conditions (Fig. 8(b)) clearly indicates an increase of $\phi'_{ss}$ with GC increment. Meanwhile, for cases where the state parameters are near zero (Fig. 8(a)) $M$ values show less dependency on GC variation (Fig. 8(a)). Further details are discussed in the following section.

## 4. Discussion

### 4.1 Micro-scale Volumetric Strain Characteristics of Gravel Soils

Triaxial tests with large strain on gravel soils in this study generally indicate a dilative tendency (Fig. 6) with an increase of GC, contrary to the typical behavior of pure or fine mixed sands (*i.e.*, contractive tendency).

Figure 9 provides a schematic comparison between the internal structural change of sand and gravel soils under shearing. Pure sands (*i.e.*, GC 0%) have a relatively high intrinsic void ratio (*e.g.*, $e_{max}$ = 0.94 and $e_{min}$ = 0.64), while gravelly sands with high GC (*i.e.*, 60%) have a more compacted inter-granular composition (*e.g.*, $e_{max}$ = 0.52 and $e_{min}$ = 0.35). In general, sandy soils require large contraction (*i.e.*, large void decrease) to achieve a steady state (Fig. 9(a)), while gravel soils with high GC (> 60%) can reach a steady state condition with a small decrease of the void ratio. Gravel soils are governed by the interlocking between gravel grains rather than sand particles, which exist inside inter-gravel voids and uncompacted (Fig. 9(b)). Consequently, for gravel soils most stress paths flow through gravel skeletons, while sand particles exist as pore fillers inside the gravel particle network. Once neighboring gravel particles are fully densified, it is no longer possible for outside sand particles to infiltrate the pore spaces of the gravel networks. Since the strengths of gravels are higher than those of sands, the shear resistances of gravel soils are finally higher than those of sandy soils.

However, although gravel soils with high GC generally have high liquefaction resistance, unusual loose cases (*e.g.*, GC = 60%, $D_r$ = 26%, and $p'_c$ = 100 kPa; Fig. 6(d)) can lead to structural collapses with positive values (*e.g.*, $\psi$ = 0.016; Table 3). Thus, the liquefaction potential of gravel soils can be more clearly defined by using state parameters.

### 4.2 Relationship between State Parameter and Liquefaction Resistance

The state parameter and liquefaction resistance (*i.e.*, $q/p'_c$) of pure and fine sands (*i.e.*, fine contents lower than 40% ~ 50%) generally show a single $\psi$ increment with $q/p'_c$ decrement, regardless of FC (Rahman and Lo, 2014; Xenaki and Athanasopoulos, 2003).

The $\psi$ and $q/p'_c$ values of gravel soils obtained from this study are plotted with previous findings on pure sands (FC 0%) and fine sands (FC 15%) (Rahman and Lo, 2014) in Fig. 10. Liquefaction resistances ($q/p'_c$) of gravel soils increase with GC increment and are generally higher than those of sandy soils (*i.e.*, FC 0% and 15%), regardless of the $\psi$ values. Moreover, the difference in the liquefaction resistance between sandy soils and gravel soils becomes larger as $\psi$ decreases.

Meanwhile, sandy soils show a wide range of state parameter values due to the high variability of particle alignment (*i.e.*, various void ratio distribution; -0.1 < $\psi$ < 0.15), while gravel soils show a narrow range (*i.e.*, -0.04 < $\psi$ < 0.02), which is more constrained with higher gravel content. Moreover, sandy soils generally show positive $\psi$ values (Rahman and Lo, 2014), while gravel soils mostly show negative $\psi$ values; this distinguishes the volume change characteristics of sandy and gravel soils where contraction dominates the stress-strain behavior of fine-sand mixtures, and vice versa for gravel soils.

The liquefaction resistance of sands is comparatively low with positive $\psi$ values, which is in accordance with the current understanding of the liquefaction characteristics of sandy soils (Rahman and Lo, 2014; Robertson, 2010). Thus, it can be concluded that most $\psi$ values of gravel soils are negative and these soils have higher liquefaction resistances than those of sandy soils. However, the approximated trends imply possibilities and conditions for liquefaction of gravel soils (*i.e.*, $\psi$ near zero or strong seismic motion surpassing the resistance). Thus, the state

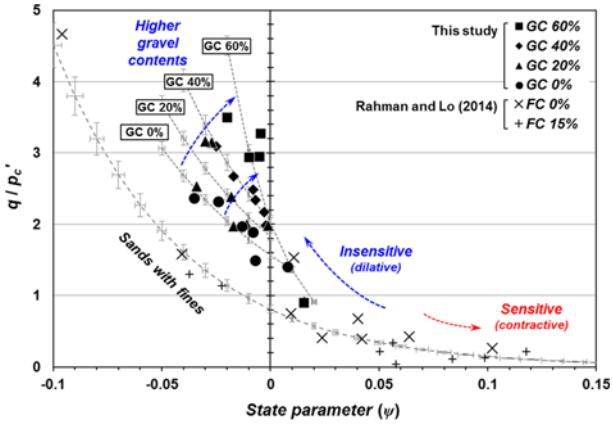


Fig. 10. Normalized Undrained Shear Strength as a Function of State Parameter

parameter and liquefaction resistance relationship of gravel soils provided in Fig. 10 can be adopted in seismic design for gravel soils to predict the liquefaction potential. A practical approach for evaluating liquefaction of gravel soils can be speculated based on Fig. 10. Two governing factors (*i.e.*, external and internal) will be considered to understand the liquefaction potential of gravel soils. Details are provided in the following section.

### 4.3 Liquefaction Potential of Gravel Soils

#### 4.3.1 In Case of Strong External Force Applied

First, a strong seismic event can induce liquefaction of gravel soils. This is related with the magnitude and frequency of motion as follows (Gutenberg and Richter, 1944):

$$\tau = \frac{1}{N} = e^{-2.303 a_{GR} + 2.303 b_{GR} M_R} \tag{2}$$

$N$ and $\tau$ are the return rate and the return period, respectively. $a_{GR}$ and $b_{GR}$ are site specific constants. Sharma *et al.* (1999) collected all seismic events on the earth. The peninsular region in India was then adopted as a study region to evaluate the relationship of magnitude-frequency, and finally $a_{GR}$ and $b_{GR}$ were suggested as 4.35 and 0.83 for Indian plate, respectively (Sharma *et al.*, 1999). Although the $a_{GR}$ and $b_{GR}$ are regional coefficients, the following application was adopted as an example for practical evaluation of liquefaction of gravel soils. As shown in Table 1, liquefaction in gravel soil deposits was reported for earthquakes having moment magnitude scales ($M_w$) and Richter scales ($M_R$) larger than 7 (Hanks and Kanamori, 1979). Accordingly, the return period ($\tau$) corresponding to $M_R$ = 7 is about 30 years (28.9 years).

Thus, unusual earthquake events (*e.g.*, 30 year return period) with massive seismic energy (*i.e.*, $M_w > 7$ or PGA > 0.2 $g$) (Table 1) have the possibility of inducing liquefaction problems in gravel soils, regardless of $\psi$ and $q/p_c'$ conditions in situ. Such catastrophic disasters are uncontrollable. On the other hand, when a smaller earthquake occurs, liquefaction also can occur with attenuation of the resistance of gravel soils. This is discussed in the following section.

#### 4.3.2 In Case of Internal Resistance Reduction

In the case of pure sands, the '*void redistribution effect*' is considered to be the most likely mechanism responsible for in-situ liquefaction (Boulanger and Truman, 1996; Kulasingam *et al.*, 2001; Whitman, 1985). Void redistribution is known to occur when relatively low permeability layers (*e.g.*, stiff clay) are located above and below a coarse layer having high permeability, and the upper and lower layers provide undrained boundary conditions (Fig. 11(a)). Thus, excessive pore water pressure can be generated during seismic motion (Fig. 11(b)). After an earthquake, dispersed gravel particles sediment down while water flows upward and forms a water film at the top of the gravel layer. As a result, the upper part of the gravel layer loosens, while the lower part of the gravel layer becomes denser

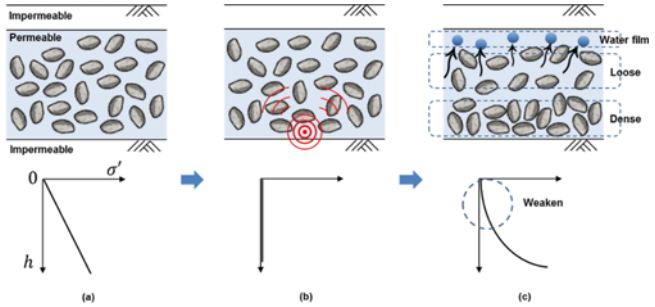


Fig. 11. Mechanism of Seismic Induced Void Redistribution: (a) Initial State before Earthquake, (b) Seismic Motion and Immediate Liquefaction (during earthquake), (c) Upward Drainage Fluid Flow, which Renders Densification (void redistribution after earthquake)

(Fig. 11(c)). This phenomenon is commonly observed in experimental approaches using dynamic geo-centrifuge modeling (Kulasingam *et al.*, 2004; Malvick *et al.*, 2008) and site characterizations (Idriss and Boulanger, 2008; Kokusho, 2003).

In the same manner, this mechanism can be applied to gravel soil systems. From the test, it is validated that the gravel soils show very small variation of the void ratio. As aforementioned in Section 3.3, some gravel soils can have a loose structure (Figs. 4(c) and 9(b)) in some situations, where liquefaction may occur. Thus, although the external force is less than the aforementioned catastrophic level, the liquefaction of gravel soils can occur as a 'post-liquefaction' phenomenon caused by this void redistribution effect.

To compare the present results with the histories of past liquefaction in gravel soils, void ratios in this study and in situ void ratios from the *Wenchuan* region in China, where landslides produced by the *Wenchuan* earthquake occurred in 2008, are shown in Fig. 12 with their gravel contents (Chang *et al.*, 2010; Chang *et al.*, 2011). The residual percent at a #4 sieve (4.75 mm) is determined as the gravel content of the sample from the grain distribution curve based on *USCS*. As shown in Fig. 12, most in situ void ratio conditions of the gravel soils in *Wenchuan* county, where liquefaction occurred, show higher values than the steady state void ratio ($e_{ss}$), even though the in-situ gravel contents were high (*i.e.*, 60% ± 20%). Thus, even though higher gravel content

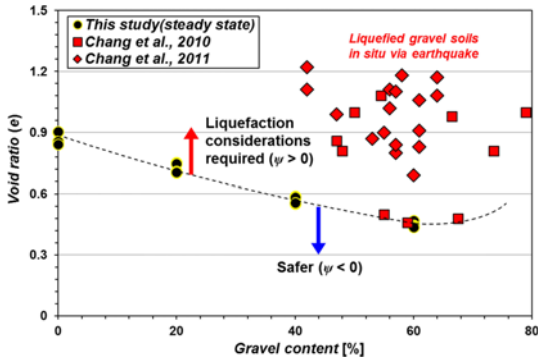


Fig. 12. Void Ratio and Gravel Content Relationship of Gravel Soils for Liquefaction Considerations

provides higher liquefaction resistance for gravel soils, liquefaction problems must be considered cautiously if the site soil compositions tend to be highly contractive (*e.g.*, high void ratio, low density) and the site is located in a critical earthquake zone (belt).

In summary, the results of this study imply that liquefaction issues must be considered for gravel soils that have uncompacted compositions and in situ undrained boundaries (*i.e.*, overburden and underlying impermeable layers) and when they are located in geological strong seismic zones.

## 5. Conclusions

The stress-strain characteristics for large-strain deformation and the liquefaction potential of gravel soils were evaluated in association with the variation in state parameters (*i.e.*, $e_{ss}$ and $\psi$) and gravel contents. Undrained static triaxial tests were performed on gravel soils with gravel content of 0, 20, 40, and 60%, various initial densities ($D_r$), and confinements ($p_c'$), respectively.

From the obtained results, the liquefaction resistance (*i.e.*, undrained shear strength) of gravel soils increases as the gravel content increases. The corresponding state parameter shows a meaningful relationship with the liquefaction resistance in gravel soils regardless of in situ conditions such as density and confinement. The state parameter varies with respect to gravel content. Gravel soils tend to be less sensitive to external loading with gravel content increases. It is concluded that the formation of strong interactions between gravel particles prevents large deformation of gravel soils before full densification. The liquefaction resistance decreases when the state parameter is positive (*i.e.*, contractive; pure sands and fine sands), while the liquefaction resistance increases when the state parameter is negative (*i.e.*, dilative; gravel sands).

Based on the results, the liquefaction potential of gravel soils has been evaluated in terms of external and internal factors. For the external factor, liquefaction can occur when strong seismic motion is applied (*e.g.*, $M_w > 7$ or PGA > 0.2 g), regardless of the soil type. However, relatively small external loading can also result in liquefaction by inducing internal resistance of gravel soils. In this research, the void redistribution effect has been asserted as the main phenomenon that attenuates gravel soils. In addition, the case history of liquefaction in gravel soils reveals that undrained conditions by overburdened impermeable layers give rise to this effect.

Overall, liquefaction in gravel soils can occur when the gravel layer is under impermeable geological conditions with contractive in situ conditions, and strong seismic loading coincides. At this time, the state parameter can be used as an effective and accurate indicator to evaluate liquefaction potential of gravel soils.

## Acknowledgements

The research described in this paper was financially supported by the grant from the Strategic Research Project (Development of Key Excavation Solutions for Expandable Urban Underground Space), funded by the Korea Institute of Civil Engineering and Building Technology (KICT) and the Korea Institute of Energy Technology Evaluation and Planning through the research project Development of hybrid substructure systems for offshore wind power (Project No. 20123010020110).

## References

Andrus, R. D. and Chung, R. M. (1995). *Ground improvement techniques for liquefaction remediation near existing lifelines*, US National Institute of Standards and Technology.

ASTM (2012). *D 1921 Standard test methods for particle size (Sieve Analysis) of plastic materials*, American Society for Testing and Materials, West Conshohocken, PA.

Been, K. and Jefferies, M. G. (1985). "A state parameter for sands." *Géotechnique*, Vol. 35, No. 2, pp. 99-112, DOI: 10.1680/geot.1985.35.2.99.

Boulanger, R. W. and Truman, S. P. (1996). "Void redistribution in sand under post-earthquake loading." *Canadian Geotechnical Journal*, Vol. 33, No. 5, pp. 829-834, DOI: 10.1139/t96-109-329.

Cao, Z., Leslie Youd, T., and Yuan, X. (2011). "Gravelly soils that liquefied during 2008 Wenchuan, China earthquake, Ms=8.0." *Soil Dynamics and Earthquake Engineering*, Vol. 31, No. 8, pp. 1132-1143, DOI: 10.1016/j.soildyn.2011.04.001.

Castro, G. and Poulos, S. J. (1977). "Factors affecting liquefaction and cyclic mobility." *Journal of the Geotechnical Engineering Division*, Vol. 103, No. 6, pp. 501-506.

Chang, D. S., Zhang, L., and Xu, Y. (2010). "Testing and analysis of erodibility of Hongshihe landslide dam." *Proc., 5th International Conference on Scour and Erosion*, ASCE, San Francisco, Vol. 1, pp. 338-347.

Chang, D. S., Zhang, L. M., Xu, Y., and Huang, R. Q. (2011). "Field testing of erodibility of two landslide dams triggered by the 12 May Wenchuan earthquake." *Landslides*, Vol. 8, No. 3, pp. 321-332, DOI: 10.1007/s10346-011-0256-x.

Evans, M., Bolton Seed, H., and Seed, R. (1992). "Membrane compliance and liquefaction of sluiced gravel specimens." *Journal of Geotechnical Engineering*, Vol. 118, No. 6, pp. 856-872, DOI: 10.1061/(ASCE)0733-9410(1992)118:6(856).

Evans, M. and Zhou, S. (1995). "Liquefaction behavior of sand-gravel composites." *Journal of Geotechnical Engineering*, Vol. 121, No. 3, pp. 287-298, DOI: 10.1061/(ASCE)0733-9410(1995)121:3(287).

Guettaya, I., El Ouni, M. R., and Moss, R. E. S. (2013). "Verifying liquefaction remediation beneath an earth dam using SPT and CPT based methods." *Soil Dynamics and Earthquake Engineering*, Vol. 53, pp. 130-144. DOI: 10.1016/j.soildyn.2013.06.009.

Gutenberg, B. and Richter, C. F. (1944). "Frequency of earthquakes in California." *Bulletin of the Seismological Society of America*, Vol. 34, No. 4, pp. 185-188.

Hanks, T. C. and Kanamori, H. (1979). "A moment magnitude scale." *Journal of Geophysical Research: Solid Earth*, Vol. 84, No. 5, pp. 2348-2350, DOI: 10.1029/JB084iB05p02348.

Hynes, M. E. (1988). *Pore pressure generation characteristics of gravel under undrained cyclic loading*, Doctoral Thesis, University of California, Berkeley.

Idriss, I. and Boulanger, R. W. (2008). *Soil liquefaction during earthquakes*, Earthquake Engineering Research Institute.

Ishihara, K. (1993). "Liquefaction and flow failure during earthquakes." *Géotechnique*, Vol. 43, No. 3, pp. 351-451, DOI: 10.1680/geot.1993.

43.3.351.

Jefferies, M. and Been, K. (2015). *Soil liquefaction: A critical state approach*, CRC Press, Boca Raton, FL, USA.

Kim, B. S. (2005). *Liquefaction behavior of gravel-sand mixtures*, Doctoral Thesis, Inha University, Incheon, South Korea.

Kokusho, T. (2003). "Current state of research on flow failure considering void redistribution in liquefied deposits." *Soil Dynamics and Earthquake Engineering*, Vol. 23, No. 7, pp. 585-603, DOI: 10.1016/S0267-7261(03)00067-8.

Kokusho, T., Hara, T., and Hiraoka, R. (2004). "Undrained shear strength of granular soils with different particle gradations." *Journal of Geotechnical and Geoenvironmental Engineering*, Vol. 130, No. 6, pp. 621-629, DOI: 10.1061/(ASCE)1090-0241(2004)130:6(621).

Kulasingam, R., Malvick, E. J., Boulanger, R. W., and Kutter, B. L. (2001). "Void redistribution and localization of shear strains in model sand slopes with silt seams: Report on first year activities." *Proc., US–Japan Joint Workshop and 3rd Grantees Meeting*, pp. 117-128.

Kulasingam, R., Malvick, E., Boulanger, R., and Kutter, B. (2004). "Strength loss and localization at silt interlayers in slopes of liquefied sand." *Journal of Geotechnical and Geoenvironmental Engineering*, Vol. 130, No. 11, pp. 1192-1202, DOI: 10.1061/(ASCE)1090-0241(2004)130:11(1192).

Ladd, R. S. (1978). "Preparing test specimens using undercompaction." *Geotechnical Testing Journal*, ASTM, Vol. 1, No. 1, pp. 16-23, DOI: 10.1520/GTJ10364J.

Lin, P.-S., Chang, C.-W., and Chang, W.-J. (2004). "Characterization of liquefaction resistance in gravelly soil: Large hammer penetration test and shear wave velocity approach." *Soil Dynamics and Earthquake Engineering*, Vol. 24, Nos. 9-10, pp. 675-687, DOI: 10.1016/j.soildyn.2004.06.010.

Malvick, E., Kutter, B., and Boulanger, R. (2008). "Postshaking shear strain localization in a centrifuge model of a saturated sand slope." *Journal of Geotechnical and Geoenvironmental Engineering,* Vol. 134, No. 2, pp. 164-174, DOI: 10.1061/(ASCE)1090-0241(2008)134:2(164).

National Research Council (1985). *Liquefaction of soils during earthquake,* National Academies.

Nicholson, P. G., Seed, R. B., and Anwar, H. A. (1993). "Elimination of membrane compliance in undrained triaxial testing. I. Measurement and evaluation." *Canadian Geotechnical Journal*, Vol. 30, No. 5, pp. 727-738, DOI: 10.1139/t93-065.

Rahman, M. and Lo, S. (2014). "Undrained behavior of sand-fines mixtures and their state parameter." *Journal of Geotechnical and Geoenvironmental Engineering*, Vol. 140, No. 7, pp. 04014036-1-12, DOI: 10.1061/(ASCE)GT.1943-5606.0001115.

Robertson, P. (2010). "Estimating in-situ state parameter and friction angle in sandy soils from CPT." *Proc., 2nd International Symposium on Cone Penetration Testing,* Huntington Beach, CA, USA.

Santamarina, J. C. and Cho, G. C. (2001). "Determination of critical state parameters in sandy soils-Simple procedure." *Geotechnical Testing Journal*, ASTM, Vol. 24, No. 2, pp. 185-192, DOI: 10.1520/GTJ11338J.

Sharma, R., Gupta, S., and Kumar, S. (1999). "Application of extreme-value distribution for estimating earthquake magnitude-frequency relationships." *ISET Journal of Earthquake Technology*, Vol. 36, No. 1, pp. 15-26.

Siddiqi, F. H. (1984). *Strength evaluation of cohesionless soils with oversize particles*, University of California, Davis, California.

Terzaghi, K., Peck, R. B., and Mesri, G. (1996). *Soil mechanics in engineering practice*, 3rd Ed. John Wiley & Sons, New York.

Wang, W. S. (1984). "Earthquake damages to earth dams and levees in relation to soil liquefaction and weakness in soft clays." *Proc., First International Conference on Case Histories in Geotechnical Engineering*, Missouri University of Science and Technology, USA, pp. 511-521.

Whitman, R. V. (1985). "On liquefaction." *Proc., 11th International Conference on Soil Mechanics and Foundation Engineering*, Balkema Rotterdam, pp. 1923-1926.

Xenaki, V. C. and Athanasopoulos, G. A. (2003). "Liquefaction resistance of sand–silt mixtures: An experimental investigation of the effect of fines." *Soil Dynamics and Earthquake Engineering*, Vol. 23, No. 3, pp. 1-12, DOI: 10.1016/S0267-7261(02)00210-5.